Universal Quantum Computation Using Atoms in Cross-Cavity Systems

Luiz Otavio Ribeiro Solak, Daniel Zini Rossatto, and Celso Jorge Villas-Boas Daniel Zini Rossatto,

¹Departamento de Física, Universidade Federal de São Carlos, 13565-905 São Carlos, São Paulo, Brazil

²Universidade Estadual Paulista (Unesp), Instituto de Ciências e Engenharia,

Campus de Itapeva, 18409-010 Itapeva, São Paulo, Brazil

Quantum gates are the building blocks of quantum circuits, which in turn are the cornerstones of quantum information processing. In this work we theoretically investigate a single-step implementation of both a universal two- (CNOT) and three-qubit (quantum Fredkin) gates in a cross-cavity setup coupled to a Λ -type three-level atom. Within a high-cooperativity regime, the system exhibits an atomic-state-dependent quantum interference involving the two-mode single-photon bright and dark states of the input light pulses. This allows for the controlled manipulation of light states by the atom and vice versa. Our results indicate these quantum gates can be implemented with high probability of success using the state-of-the-art parameters, either for the weak- or strong-coupling regime, where the quantum interference is due to an electromagnetically-induced-transparency-like phenomenon and the Autler-Townes splitting, respectively. This work not only paves the way for implementing quantum gates in a single step using simple resources, thus avoiding the need to chain basic gates together in a circuit, but it also endorses the potential of cross-cavity systems for realizing universal quantum computation.

Introduction.—Efficient manipulation of quantum information is crucial for the realization of quantum computers [1], which can improve the performance of computing tasks [2] or even solve problems that are intractable for classical computers [3]. A quantum computation is carried out through a quantum circuit composed of a sequence of quantum operations, such as quantum gates, measurements and initialization of qubits [4]. However, the implementation of a multiqubit gate in the standard circuit model remains challenging because it needs to be decomposed into a chain of universal quantum gates, comprising single- and two-qubit basic gates [4]. For example, implementing a three-qubit quantum Fredkin gate requires at least five two-qubit gates [5]. This gate is fundamental for universal reversible computation as it plays important roles in quantum computing [6-8], quantum cryptography [9, 10], quantum error correction [11, 12] and measurement [13, 14]. Therefore, it is of interest to implement this gate more directly [15, 16], without decomposition, in order to mitigate the resource overhead, thus enhancing the overall probability of success to implement it.

Various physical systems are currently being explored as potential candidates for the implementation of large-scale universal quantum computing [6, 17–20]. In particular, we are interested in cavity-based quantum networks with single atoms in optical cavities [20–27], in which a variety of applications were proposed as well as performed, such as secure information sharing [28, 29], quantum memory [30–32], quantum transistors [33] and quantum gate implementation [34–41].

In this Letter we show a single-step implementation of both a universal two- (CNOT) and three-qubit (quantum Fredkin) gates in a cross-cavity setup [27] with single-sided cavities, with their semitransparent mirrors coupled to a continuum of free-space modes. These modes act as bosonic reservoirs that are used both to impinge single-photon pulses upon the cavities (a and b) and to measure the output fields that emerge from the system. In addition, a Λ -type three-level atom (two metastable ground states, $|g_1\rangle$ and $|g_2\rangle$, and an excited one

 $|e\rangle$) is trapped inside the cavity setup. For our purposes, the atomic transition $|g_1\rangle\leftrightarrow|e\rangle$ is resonantly coupled to both intracavity modes, while the atomic ground state $|g_2\rangle$ remains uncoupled. A schematic representation of the system is illustrated in Fig. 1(a).

Using this architecture, we investigated a protocol in which the output fields that emerge from the cavities are conditioned on the atomic state. In a high-cooperativity regime, if the atom is in $|g_1\rangle$ and a single-photon pulse impinges upon the cavity a (or b), the light states between the cavities are exchanged due to a quantum interference involving dark and bright states, resulting in an output single-photon pulse transmitted by the opposite cavity [Fig. 1(b) and 1(e)]. If the atom is in $|g_2\rangle$, it becomes transparent to the cavity modes, and thus the output single-photon pulse exits from the same cavity through which the input pulse entered [Fig. 1(c)].

Therefore, depending on the atomic population, the system performs controlled operations on the external fields. For instance, considering the *control* qubit by means of the atomic ground states $|g_1\rangle \to |\overline{1}\rangle_c$ and $|g_2\rangle \to |\overline{0}\rangle_c$, the system performs a CNOT gate (two-qubit gate) when the target qubit is defined through the two-mode reservoir states with a single photon $|1\rangle_{\alpha}\otimes|0\rangle_{\beta}\rightarrow|\bar{1}\rangle$ and $|0\rangle_{\alpha}\otimes|1\rangle_{\beta}\rightarrow|\bar{0}\rangle$. The system can also implement a Fredkin gate (three-qubit gate) when we consider the two target qubits via $|1\rangle_{\alpha} \rightarrow |\overline{1}\rangle_{a}$, $|1\rangle_{\beta} \rightarrow |\bar{1}\rangle_{b}$ (analogously for $|\bar{0}\rangle_{a,b}$), as summarized in the truth table shown in Fig. 1(d). Here $|1\rangle_{\alpha}$ and $|1\rangle_{\beta}$ represent the single-photon state of the input/output pulses of cavities a and b ($|0\rangle_{\alpha}$ and $|0\rangle_{\beta}$ are the vacuum states), respectively. Consequently, universal quantum computation [4] can be performed by using this cross-cavity setup in combination with single-qubit operations.

It is worth emphasizing that, when the system works in a high-cooperativity regime, the quantum gates can be implemented not only due to the Autler-Townes splitting [42] in the strong-coupling regime, but also in the weak-coupling regime because of an electromagnetically-induced-transparency-like

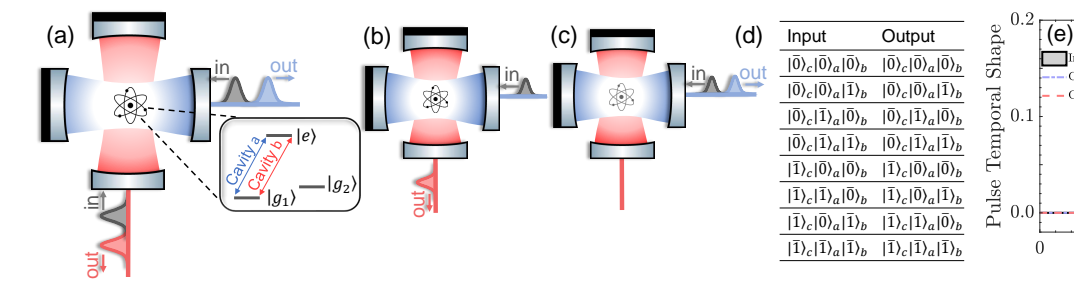


FIG. 1. (a) Pictorial illustration of a Λ -type three-level atom resonantly coupled to a cross-cavity system, with single-sided cavities. (b) Impinging a single-photon pulse upon a cavity when the atom is in $|g_1\rangle$, a quantum interference exchanges the cavity light states, resulting in a single-photon pulse transmitted by the opposite cavity. (c) If the atom is is $|g_2\rangle$, it becomes transparent to the cavities, and thus the output single-photon pulse exits from the same cavity through which it entered. (d) Truth table of the Fredkin gate implemented by our system, where the control qubit is given by the atomic ground states ($|g_1\rangle \to |\bar{1}\rangle_c$ and $|g_2\rangle \to |\bar{0}\rangle_c$), while the target qubits are given by the vacuum and single-photon states of the reservoirs of cavity a and b: $|\bar{0}\rangle_a$, $|\bar{1}\rangle_a$ and $|\bar{0}\rangle_b$, $|\bar{1}\rangle_b$. (e) Dynamics when a single-photon pulse of temporal shape $\alpha_{\rm in}(t)$ impinges upon the cavity a, but leaves from cavity b [$\beta_{\rm out}(t)$] since the atom is in $|g_1\rangle$.

phenomenon [43–45].

Model.—To assess the realization of the aforementioned quantum gates, let us analyze the system response under various parameter regimes. The setup in Fig. 1(a), in an interaction picture rotating at the cavities resonant frequency (ω_c), and under the *white-noise limit* [46], is described by ($\hbar = 1$)

$$H = \int_{-\infty}^{\infty} d\omega \, \omega A_{\omega}^{\dagger} A_{\omega} + \int_{-\infty}^{\infty} d\omega \, \omega B_{\omega}^{\dagger} B_{\omega}$$

$$+ \frac{i}{\sqrt{\pi}} \int_{-\infty}^{\infty} d\omega \left[\sqrt{\kappa_a} (a^{\dagger} A_{\omega} - a A_{\omega}^{\dagger}) + \sqrt{\kappa_b} (b^{\dagger} B_{\omega} - b B_{\omega}^{\dagger}) \right]$$

$$+ \underbrace{(g_a a + g_b b) \sigma_+^1 + (g_a^* a^{\dagger} + g_b^* b^{\dagger}) \sigma_-^1}_{H_{\text{sys}}}, \tag{1}$$

in which $\sigma_+^1 = |e\rangle\langle g_1|$ and $\sigma_-^1 = |g_1\rangle\langle e|$ are atomic ladder operators, a and b (a^\dagger and b^\dagger) are the annihilation (creation) operators of the intracavity modes, while A_ω and B_ω (A_ω^\dagger and B_ω^\dagger) are the frequency-dependent annihilation (creation) operators [47] of the bosonic reservoirs of cavities a and b, respectively. Here, κ_a and κ_b stand for the decay rates of the field amplitudes of cavities a and b, respectively. They establish the coupling between external and intracavity modes. Finally, g_a and g_b are the coupling strength between the atomic transition $|g_1\rangle\leftrightarrow|e\rangle$ and the intracavity modes.

To evolve this system, we consider an initial state that includes all possible inputs for the two- and three-qubit operations under consideration

$$|\Psi(t_{0})\rangle = \underbrace{(\lambda_{1}|g_{1}\rangle + \lambda_{2}|g_{2}\rangle)}_{\text{Atom}} \otimes \underbrace{(|0\rangle_{a} \otimes |0\rangle_{b})}_{\text{Cavities}}$$

$$\otimes \underbrace{(\mu_{a}|1\rangle_{\alpha} \otimes |0\rangle_{\beta} + \mu_{b}|0\rangle_{\alpha} \otimes |1\rangle_{\beta} + \mu_{c}|1\rangle_{\alpha} \otimes |1\rangle_{\beta})}_{\text{Reservoirs}}, \quad (2)$$

in which $|1\rangle_{\alpha}=\int_{-\infty}^{\infty}d\omega\xi_{\rm in}(\omega)A_{\omega}^{\dagger}|0\rangle_{\alpha}$ describes the input field in a continuous-mode single-photon state [47] impinging upon the cavity a, and $|1\rangle_{\beta}=\int_{-\infty}^{\infty}d\omega\zeta_{\rm in}(\omega)B_{\omega}^{\dagger}|0\rangle_{\beta}$ the

analog for cavity b. The Fourier transform of the spectral density function of the pulses, $\xi_{\rm in}(\omega)$ and $\zeta_{\rm in}(\omega)$, provides the square-normalized temporal shape of the incoming pulses, $\alpha_{\rm in}(t)$ and $\beta_{\rm in}(t)$ [47], while the coefficients λ_k (k=1,2) and μ_p (p=a,b,c) are related to the initial probability of the respective state. Hereafter, the tensor product will be omitted for the sake of simplicity.

100

Methods.—The system response can be investigated via the input-output theory [48], with output and input operators

$$z_{\text{out}}(t) = +\frac{1}{\sqrt{2\pi}} \int_{-\infty}^{\infty} d\omega e^{-i\omega(t - t_{\text{out}})} \underbrace{Z_{\omega}(t_{\text{out}})}_{z_{\text{out}}(\omega)}, \quad (3)$$

$$z_{\rm in}(t) = -\frac{1}{\sqrt{2\pi}} \int_{-\infty}^{\infty} d\omega e^{-i\omega(t - t_{\rm in})} \underbrace{Z_{\omega}(t_{\rm in})}_{z_{\rm in}(\omega)}, \tag{4}$$

for $\{z=a,Z=A\}$ and $\{z=b,Z=B\}$, with $t_{\rm in}\to -\infty$ and $t_{\rm out}\to +\infty$. The boundary condition relating the far-field amplitude outside each cavity to its corresponding intracavity field is given by the input-output relation [48]

$$z_{\text{out}}(t) = \sqrt{2\kappa_z} \, z(t) - z_{\text{in}}(t). \tag{5}$$

In addition, from Eqs. (1) and (4), we have the Heisenberg-Langevin equation for an arbitrary system operator $\mathcal{O}(t)$ [46]

$$\dot{\mathcal{O}} = -i[\mathcal{O}, H_{\text{sys}}] - \sum_{l=1}^{2} \Gamma_{l}([\mathcal{O}, \sigma_{+}^{l}] \sigma_{-}^{l} - \sigma_{+}^{l}[\mathcal{O}, \sigma_{-}^{l}])
- \sum_{z=a}^{b} [\mathcal{O}, z^{\dagger}] (\kappa_{z} z - \sqrt{2\kappa_{z}} z_{\text{in}})
+ \sum_{z=a}^{b} (\kappa_{z} z^{\dagger} - \sqrt{2\kappa_{z}} z_{\text{in}}^{\dagger}) [\mathcal{O}, z],$$
(6)

in which Γ_l is the decay rate of the atomic spontaneous emission associated with the transition $|e\rangle \rightarrow |g_l\rangle$, and $\sigma_+^l = (\sigma_-^l)^\dagger = |e\rangle\langle g_l|$. Note that the coupling of each atomic transition to its respective reservoir was also considered in Eq. (6) [omitted in Eq. (1)], establishing the exclusive source of photon loss considered in our setup. However, without loss of

generality, we suppress the input operators for these reservoirs as they are assumed to be initially in the vacuum state.

Although it is possible to construct a finite set of coupled dynamical equations for the system operators based on Eq. (6), it is generally nonlinear and challenging to solve. However, it becomes linear by applying the Holstein-Primakoff approximation $\sigma_z = \sigma_+^1 \sigma_-^1 - \sigma_-^1 \sigma_+^1 \approx -1$ [49], which holds as long as the atom is rarely excited and becomes exact if the atom only populates $|g_2\rangle$ or $g_a = g_b = 0$. Thus,

$$\dot{a}(t) = -ig_a^* \sigma_-^1(t) - \kappa_a a(t) + \sqrt{2\kappa_a} a_{\rm in}(t), \qquad (7)$$

$$\dot{b}(t) = -ig_b^* \sigma_-^1(t) - \kappa_b b(t) + \sqrt{2\kappa_b} b_{\rm in}(t),$$
 (8)

$$\dot{\sigma}_{-}^{1}(t) = -i[g_{a}a(t) + g_{b}b(t)] - \Gamma\sigma_{-}^{1}(t), \tag{9}$$

with $\Gamma = \Gamma_1 + \Gamma_2$. In this scenario, an analytical inputoutput relation for the field amplitudes in the frequency domain can be derived by taking the Fourier transform of Eq. (5) and Eqs. (7)–(9). For instance, setting (just for convenience) $g_a = -g_b \equiv g \in \mathbb{R}$ and $\kappa_a = \kappa_b \equiv \kappa$,

$$a_{\text{out}}^{\dagger}(\omega) = r_{\omega} a_{\text{in}}^{\dagger}(\omega) + t_{\omega} b_{\text{in}}^{\dagger}(\omega),$$
 (10)

$$b_{\text{out}}^{\dagger}(\omega) = t_{\omega} a_{\text{in}}^{\dagger}(\omega) + r_{\omega} b_{\text{in}}^{\dagger}(\omega),$$
 (11)

where r_{ω} and t_{ω} are the (frequency- and atomic-state-dependent) complex reflection and transmission coefficients, respectively (see Supplemental Material [50]). For resonant incoming fields, which will be employed throughout this study, the system response is

$$r_{\omega=\omega_c} = \frac{1}{1+4C} |g_1\rangle\langle g_1| + |g_2\rangle\langle g_2|, \qquad (12)$$

$$t_{\omega=\omega_c} = \frac{4C}{1+4C} |g_1\rangle\langle g_1|, \tag{13}$$

in which $C=g^2/2\kappa\Gamma$ is the cooperativity parameter. It is also worth examining the system response through the collective-mode operators $X^{\pm}_{\rm in(out)}(\omega)=[a_{\rm in(out)}(\omega)\pm b_{\rm in(out)}(\omega)]/\sqrt{2}$,

$$X_{\text{out}}^+(\omega_c) = X_{\text{in}}^+(\omega_c),\tag{14}$$

$$X_{\text{out}}^{-}(\omega_c) = \left(\frac{1 - 4C}{1 + 4C} |g_1\rangle\langle g_1| + |g_2\rangle\langle g_2|\right) X_{\text{in}}^{-}(\omega_c).$$
 (15)

We stress that the results above are valid only when the excited state population is negligible. In a parameter regime beyond the validity of the Holstein-Primakoff approximation (atom can be significantly excited), it is advantageous to work with the dynamical equations for the average values of the operators in Eq. (6). The resulting set is linear but infinite, however it can become finite but nonlinear by applying the semiclassical mean-field approximation [51] (factorization of the average values of two operators, e.g., $\langle \sigma a \rangle \approx \langle \sigma \rangle \langle a \rangle$), culminating in a set of dynamical equations for $\langle a \rangle$, $\langle b \rangle$, $\langle \sigma_-^1 \rangle$, $\langle \sigma_z \rangle$ and $\langle \sigma_{ee} \rangle$, with $\sigma_{ee} = |e\rangle \langle e|$ (see Supplemental Material [50]). The solution to the semiclassical dynamical equations can be obtained numerically without difficulty, even if there are many atoms inside the cross-cavity setup. Nonetheless, this solution neglects the correlation between the atom

and the intracavity fields, and assumes the external fields as classical ones (coherent pulses), such that $\langle a_{\rm in}\rangle=\alpha_{\rm in}(t)$ and $\langle b_{\rm in}\rangle=\beta_{\rm in}(t).$ Both analytical and semiclassical approaches will be used here to compare them with the quantum description of the setup outlined below. This analysis allowed us to investigate the influence of nonlinearities and quantum correlations on the attainment of a CNOT or a Fredkin gate in this system.

When the initial state described in Eq. (2) contains only a single excitation (i.e., $\mu_c = 0$), an exact quantum approach for the system dynamics, excluding the occurrences of photon loss due to spontaneous atomic emission, can be obtained by numerically solving the Schrödinger equation $i\partial_t |\Psi(t)\rangle = H_{\text{eff}} |\Psi(t)\rangle$, with $H_{\text{eff}} = H_{\text{sys}} - i\Gamma\sigma_{ee}$ [52]. In this scenario, which allows describing the CNOT gate operations at least, the temporal shapes of the output pulses emerging from cavity $a \left[\alpha_{\text{out}}^l(t)\right]$ and $b \left[\beta_{\text{out}}^l(t)\right]$, conditioned to the atomic state $|g_l\rangle$, are determined using the input-output relations $\alpha_{\mathrm{out}}^l(t) = \sqrt{2\kappa_a}c_a^l(t) - \alpha_{\mathrm{in}}^l(t)$ and $\beta_{\mathrm{out}}^l(t) = \sqrt{2\kappa_b}c_b^l(t) - \beta_{\mathrm{in}}^l(t)$, with $\alpha_{\mathrm{in}}^l(t) = \lambda_l\mu_a\alpha_{\mathrm{in}}(t)$ and $\beta_{\rm in}^l(t) = \lambda_l \mu_b \beta_{\rm in}(t)$, c_a^l and c_b^l being the probability amplitudes of finding a single excitation inside the cavity a and b, respectively, while the atom is in $|g_l\rangle$ and the other modes are in the vacuum state (see Supplemental Material [50]). The non-Hermitian nature of H_{eff} results in an unnormalized state $|\Psi(t)\rangle$, such that $(1-\int_{-\infty}^{\infty} |\langle \Psi(t)|\Psi(t)\rangle|^2 dt)$ quantifies the probability of losing the input single photon due to atomic spontaneous emission, corresponding to the failure probability of the CNOT gate. Here, we describe the input pulse as a Gaussian wave packet that contains a single photon, $\alpha_{\rm in}(t)$ or $\beta_{\rm in}(t)=(\eta\sqrt{\pi})^{-\frac{1}{2}}\exp[-\frac{1}{2}\frac{(t-t_0)^2}{\eta^2}]$, in which t_0 is the time when its maximum arrives at the cavity semitransparent mirror and the pulse duration is determined by $\tau_p = 2\eta \sqrt{2 \ln(2)}$.

To conclude our analysis, it only remains to determine an exact solution for the system dynamics associated with the three-qubit operation with one incoming single-photon pulse for each cavity [$\mu_a = \mu_b = 0$ and $\mu_c = 1$ in Eq. (2)]. However, the previous method leads to a set of integro-differential equations that becomes challenging to solve as we increase the number of excitations in the setup. To circumvent that, we opted to employ an alternative method to investigate the exact system response when the input field is in the state $|1\rangle_{\alpha}|1\rangle_{\beta}$. Although this method is numerically feasible, it is computationally demanding, because it involves solving a set of hierarchical master equations [53],

$$\dot{\varrho}_{m,n;p,q}(t) = -i \left[H_{\text{sys}}, \varrho_{m,n;p,q} \right]
+ \sqrt{m} \alpha_{\text{in}}(t) \left[\varrho_{m-1,n;p,q}, L_{a}^{\dagger} \right] + \sqrt{p} \beta_{\text{in}}(t) \left[\varrho_{m,n;p-1,q}, L_{b}^{\dagger} \right]
+ \sqrt{n} \alpha_{\text{in}}^{*}(t) \left[L_{a}, \varrho_{m,n-1;p,q} \right] + \sqrt{q} \beta_{\text{in}}^{*}(t) \left[L_{b}, \varrho_{m,n;p,q-1} \right]
+ \sum_{z=a}^{b} \mathcal{L}[L_{z}] \varrho_{m,n;p,q} + \sum_{j=1}^{2} \mathcal{L}[L_{j}] \varrho_{m,n;p,q},$$
(16)

in which $L_z = \sqrt{2\kappa_z} z$ and $L_j = \sqrt{2\Gamma_j} \sigma_-^j$, with $\mathcal{L}[L]\varrho = L^{\dagger}\varrho L - (L^{\dagger}L\varrho + \varrho L^{\dagger}L)/2$. For the two-photon initial state under consideration, the system dynamics is described by

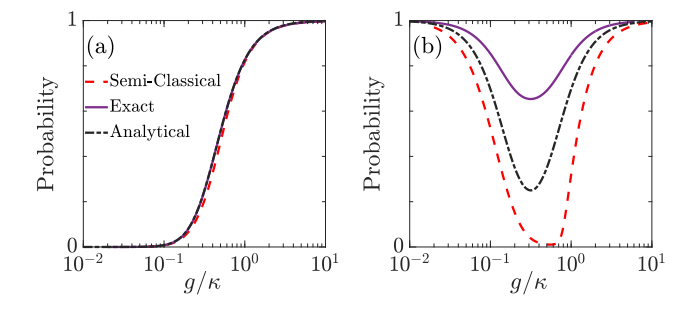


FIG. 2. Comparison among the analytical, semiclassical and exact approaches for the probabilities related to (a) $|g_1\rangle|0\rangle_{\alpha}|1\rangle_{\beta} \rightarrow |g_1\rangle|1\rangle_{\alpha}|0\rangle_{\beta}$ and (b) $|g_1\rangle|1\rangle_{\alpha}|1\rangle_{\beta} \rightarrow |g_1\rangle|1\rangle_{\alpha}|1\rangle_{\beta}$ operations, using $\Gamma=0.2\kappa$ and $\kappa\tau_p=40$.

 $\varrho_{1,1;1,1}(t)$ with the initial conditions for the hierarchical master equations given by $\varrho_{m,n;p,q}(0)=\rho_{\rm sys}(0)$ if m=n and p=q, being $\varrho_{m,n;p,q}(0)=0$ otherwise. Here, $\rho_{\rm sys}(0)$ is the density matrix of the system initial state related to the first line of Eq. (2). The mean photon flux of the output fields are $\langle a_{\rm out}^\dagger(t)a_{\rm out}(t)\rangle=\mathbb{E}_{1,1;1,1}[L_a^\dagger L_a]+\alpha_{\rm in}^*(t)\mathbb{E}_{0,1;1,1}[L_a]+\mathbb{E}_{1,0;1,1}[L_a^\dagger]+|\alpha_{\rm in}(t)|^2$ and $\langle b_{\rm out}^\dagger(t)b_{\rm out}(t)\rangle=\mathbb{E}_{1,1;1,1}[L_b^\dagger L_b]+\beta_{\rm in}^*(t)\mathbb{E}_{1,1;0,1}[L_b]+\mathbb{E}_{1,1;1,0}[L_b^\dagger]+|\beta_{\rm in}(t)|^2, \ \ {\rm in} \ \ \ {\rm which} \ \mathbb{E}_{m,n;p,q}[L]={\rm Tr}_{\rm sys}[\rho_{m,n;p,q}^\dagger L].$

Results.—Hereafter we assume $g_a = -g_b \equiv g \in \mathbb{R}$, $\Gamma_1 = \Gamma_2$ and $\kappa_a = \kappa_b \equiv \kappa$, unless stated otherwise. First, note that any operation for which the atom populates $|g_2\rangle (|g_2\rangle|\psi\rangle_{\rm in} \rightarrow |g_2\rangle|\psi\rangle_{\rm out})$ invariably succeeds, since this state is not coupled to the cavity modes. In this case, Eq. (12) gives $r_{\omega=\omega_c}=1$, therefore the system operates as two independent empty cavities, and as we have considered atomic spontaneous emission as the exclusive source of photon loss, this means that the output pulse exits from the same cavity through which the input pulse entered [54]. In addition, regardless the atomic state, the operations involving $|\psi\rangle_{\rm in}=|0\rangle_{\alpha}|0\rangle_{\beta}$ also succeed due to its trivial dynamics.

Then, to complete our analysis, let us examine the probabilities of operations involving $|g_1\rangle$. Both the CNOT and Fredkin gates proposed here contain the operations $|g_1\rangle|0\rangle_{\alpha}|1\rangle_{\beta}$ $|g_1\rangle|1\rangle_{\alpha}|0\rangle_{\beta}$ and $|g_1\rangle|1\rangle_{\alpha}|0\rangle_{\beta} \rightarrow$ $|g_1\rangle|0\rangle_{\alpha}|1\rangle_{\beta}$. From Eqs. (12)and (13), the analytical probability of their occurrence is $|\langle g_1|\langle 0|_{\alpha}\langle 0|_{\beta}a_{\text{out}}(\omega_c)b_{\text{in}}^{\dagger}(\omega_c)|0\rangle_{\alpha}|0\rangle_{\beta}|g_1\rangle|^2$ $|\langle g_1|t_{\omega=\omega_c}|g_1\rangle|^2=[4C/(1+4C)]^2$. For comparison purposes, Figure 2(a) exhibits the analytical result alongside the semiclassical $(\int_{-\infty}^{\infty} dt \, |\langle a_{\text{out}}(t) \rangle|^2)$ and exact $(\int_{-\infty}^{\infty} dt \, |\alpha_{\text{out}}^1(t)|^2)$ results as a function of g/κ , considering $\Gamma = 0.2\kappa$. It is worth noting the equivalence in all treatments, which is expected since there is only one excitation throughout the process, and there are no appreciable light-matter correlations, leading to an approximate linear-optics regime for the given set of parameters. For the two-photon operation $|g_1\rangle|1\rangle_{\alpha}|1\rangle_{\beta}$ \rightarrow we obtain the analytical probability $|g_1\rangle|1\rangle_{\alpha}|1\rangle_{\beta}$, $|\langle g_1|\langle 0|_{\alpha}\langle 0|_{\beta}a_{\rm out}(\omega_c)b_{\rm out}(\omega_c)a_{\rm in}^{\dagger}(\omega_c)b_{\rm in}^{\dagger}(\omega_c)|0\rangle_{\alpha}|0\rangle_{\beta}|g_1\rangle|^2 =$

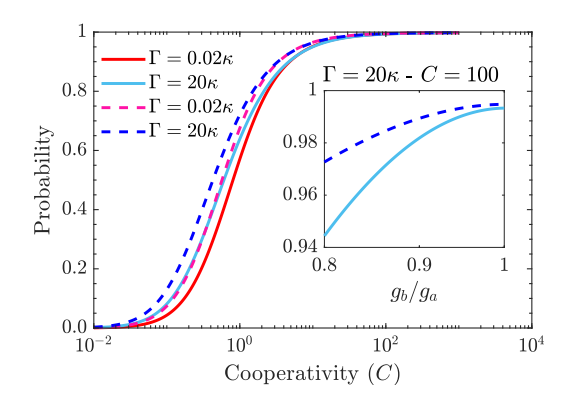


FIG. 3. Regarding the CNOT gate, probabilities as a function of the cooperativity C, for different values of total atomic spontaneous decay Γ , related to the operations $|g_1\rangle|0\rangle_{\alpha}|1\rangle_{\beta} \rightarrow |g_1\rangle|1\rangle_{\alpha}|0\rangle_{\beta}$ (or $|g_1\rangle|1\rangle_{\alpha}|0\rangle_{\beta} \rightarrow |g_1\rangle|0\rangle_{\alpha}|1\rangle_{\beta}$) with the atom as the control qubit (solid lines), and $|\Psi_B^R\rangle|\bar{1}\rangle \rightarrow |\Psi_B^R\rangle|\bar{0}\rangle$ (or $|\Psi_B^R\rangle|\bar{0}\rangle \rightarrow |\Psi_B^R\rangle|\bar{1}\rangle$) with the two modes as a control qubit. In the inset we show the sensitivity of the fidelity to deviations in the values of g_a compared to g_b . Here we set $\kappa\tau_p=40$.

 $|\langle g_1|(t_{\omega=\omega_c}^2+r_{\omega=\omega_c}^2)|g_1\rangle|^2=[1+(4C)^2]^2/(1+4C)^4, \text{ as shown in Fig. 2(b), where the exact } (\int_{-\infty}^\infty dt dt' \langle a_{\text{out}}^\dagger(t)a_{\text{out}}(t)b_{\text{out}}^\dagger(t')b_{\text{out}}(t')\rangle) \text{ [55]} \text{ and semiclassical } (\int_{-\infty}^\infty dt \, |\langle a_{\text{out}}(t)\rangle|^2 \int_{-\infty}^\infty dt' \, |\langle b_{\text{out}}(t')\rangle|^2) \text{ results are also plotted. We observe that all approaches also exhibit similar results for both low- and high-cooperativity regimes in this case. However, there is a discrepancy in the intermediate-cooperativity regime, highlighting the impact of nonlinearities and quantum correlations introduced by the presence of two photons in this process.$

The system behavior can be more elegantly and clearly described using the dark and bright states of light, which can be defined in terms of the symmetric and antisymmetric collective-mode operators [56, 57]. For the subspace of N photons, they are $|\Psi^N_{\mathcal{D}}\rangle = \frac{(X^+)^N}{\sqrt{N!}}|0\rangle|0\rangle$ and $|\Psi^N_{\mathcal{B}}\rangle =$ $\frac{(X^-)^N}{\sqrt{N!}}|0\rangle|0\rangle$, respectively. Equation (14) confirms that the input field in a dark state does not interacts with the atom regardless its state (empty-cavity scenario), then $|g_i\rangle|\Psi_{\mathcal{D}}^N\rangle_{\text{in}} \rightarrow$ $|g_j\rangle|\Psi_{\mathcal{D}}^N\rangle_{\text{out}}$. On the other hand, when the input field is in a bright state, although we also expect an empty-cavity scenario if the atom is in $|g_2\rangle$, in a high-cooperativity regime the output pulse acquires a phase $(-1)^N$ if the atom is in $|g_1\rangle$, that is, $|g_j\rangle|\Psi^N_{\mathcal{B}}\rangle_{\mathrm{in}}\to (-1)^{jN}|g_j\rangle|\Psi^N_{\mathcal{B}}\rangle_{\mathrm{out}}$. In this context, we observe another fascinating aspect of this system, which is the implementation of a CNOT gate with the control qubit defined by means of the single-photon dark and bright states of light, $|\bar{0}\rangle_c \equiv |\Psi_D^1\rangle = (|1\rangle_\alpha |0\rangle_\beta + |0\rangle_\alpha |1\rangle_\beta)/\sqrt{2}$ and $|\bar{1}\rangle_c \equiv |\Psi_B^1\rangle = (|1\rangle_\alpha |0\rangle_\beta - |0\rangle_\alpha |1\rangle_\beta)/\sqrt{2}$, whereas the target qubit is defined through the atomic superposition states $|\bar{0}\rangle \equiv (|g_2\rangle + |g_1\rangle)/\sqrt{2}$ and $|\bar{1}\rangle \equiv (|g_2\rangle - |g_1\rangle)/\sqrt{2}$.

Figure 3 shows the exact probability for the occurrence of the operation $|\bar{1}\rangle_c|\bar{0}\rangle \to |\bar{1}\rangle_c|\bar{1}\rangle$ (identical result for $|\bar{1}\rangle_c|\bar{1}\rangle \to |\bar{1}\rangle_c|\bar{0}\rangle$) when considering both the atom controlling the light

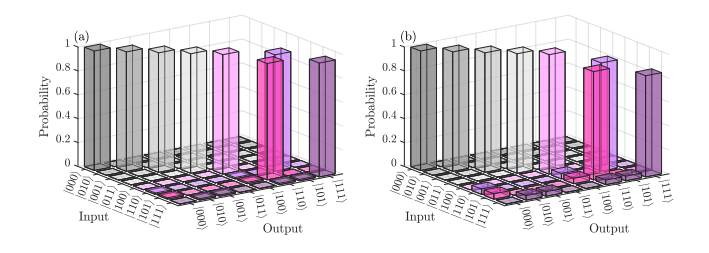


FIG. 4. Probabilities of the Fredkin gate operations for (a) C=20 and (b) C=5, considering $\Gamma=0.2\kappa$ and $\kappa\tau_p=40$.

states (solid lines) and vice versa (dashed lines), for low ($\Gamma=0.02\kappa$) and high ($\Gamma=20\kappa$) atomic spontaneous emission rates. This analysis summarizes the probability of success for implementing the CNOT gate, as only these operations do not have a unitary fidelity for all ranges of parameters in this case. We observe a probability greater than 95% for $C\gtrsim 10$. Remarkably, this high probability occurs not only for the strong-coupling regime ($\Gamma=20\kappa$ and $C\sim 10\Rightarrow g=20\kappa$), where the reflection of the input pulse in a bright state is expected when the atom is in $|g_1\rangle$ due to the Autler-Townes splitting [42], but also for the weak-coupling regime ($\Gamma=0.02\kappa$ and $C\sim 10\Rightarrow g\approx 0.6\kappa$), where the reflection of such an input pulse is due to a destructive quantum interference between the system absorption paths (electromagnetically-induced-transparency-like phenomenon) [43–45].

In the inset of Fig. 3, we show that the success probability of performing a CNOT gate decreases as the value of g_a deviates from the one of q_b (similar result is observed for deviations between the values of κ_a and κ_b). Such a deviation leads to a change in the form of the bright and dark states, then the quantum interference is no longer totally achieved, decreasing the success probability of performing the CNOT gate. Nonetheless, we observe that a high probability still holds for small deviations between the values of g_a and g_b in the regime of high cooperativity. It is worth emphasizing that our proposal for the implementation of a CNOT gate comprises a (two-mode) photonic qubit that always contain a single photon. This is an advantage over protocols that use single-mode photonic qubits because, in our case, every time the detectors do not count a photon, we know the photon was lost and then we can disregard such an event.

Finally, Figure 4 illustrates the probability of occurrence for every input-output operations present in the implementation of a Fredkin gate [truth table in Fig. 1(d)], considering $\kappa \tau_p = 40$ and $\Gamma = 0.2\kappa$ for two experimentally feasible values of cooperativity [27], C = 5 [Fig. 4(b)] and C = 20 [Fig. 4(a)]. We observe a success probability greater than 90% for C = 20. However, we can notice a decrease of that for C = 5, where the losses by atomic emission become evident, mostly for the operation involving two photons.

Conclusions.—We have shown that a cross-cavity system coupled to a Λ -type three-level atom provides a promising platform to perform universal quantum computation. We demonstrated how to implement a CNOT gate based on a

quantum interference involving bright and dark states of light, which is activated depending on the atomic state. In this case we have considered the two modes sharing a single photon as a single logic qubit. We can have either the atom controlling the light states or vice versa. In the first case, the atom operates as the control qubit, and the external two-mode light pulse in a single-photon state as the target qubit. In the second case, the control qubit is defined by the single-photon dark and bright states of the external two-mode light pulse, while the target qubit is determined by the symmetric and antisymmetric superpositions of the atomic ground states. Remarkably, we have shown that a quantum Fredkin gate can also be directly implemented with this system (without decomposing it into the basic single- and two-qubit gates), where the atom controls the light states of both pulses interacting with the cavities. In this case, each mode (in the either vacuum or single-photon states) represents a logic qubit. Based on the state-of-the-art parameters [27], our results predict high success probability for the two- and three-qubit quantum gates investigated in this study. Although we have primarily explored the optical domain and atomic systems, it is important to highlight that the principles and techniques discussed here can be adapted and extended to solid-state-based systems, such as superconducting circuits [58]. Therefore, our results contribute to the advancement of quantum technologies for applications in quantum information, communication, and computation.

We acknowledge discussions in the earlier stage of this work with Prof. Dr. Gerhard Rempe and the fruitful discussions with Prof. Dr. Antonio S. M. de Castro. This work was supported by the São Paulo Research Foundation (FAPESP, Grants Nos. 2019/11999-5, 2018/22402-7, and 2022/00209-6) and by the Brazilian National Council for Scientific and Technological Development (CNPq, Grants Nos. 311612/2021-0 and 465469/2014-0).

T. D. Ladd, F. Jelezko, R. Laflamme, Y. Nakamura, C. Monroe, and J. L. O'Brien, Quantum computers, Nature (London) 464, 45 (2010).

^[2] T. Monz, D. Nigg, E. A. Martinez, M. F. Brandl, P. Schindler, R. Rines, S. X. Wang, I. L. Chuang, and R. Blatt, Realization of a scalable shor algorithm, Science 351, 1068 (2016).

^[3] H.-S. Zhong, H. Wang, Y.-H. Deng, M.-C. Chen, L.-C. Peng, Y.-H. Luo, J. Qin, D. Wu, X. Ding, Y. Hu, P. Hu, X.-Y. Yang, W.-J. Zhang, H. Li, Y. Li, X. Jiang, L. Gan, G. Yang, L. You, Z. Wang, L. Li, N.-L. Liu, C.-Y. Lu, and J.-W. Pan, Quantum computational advantage using photons, Science 370, 1460 (2020).

^[4] M. A. Nielsen and I. Chuang, Quantum computation and quantum information (Cambridge University Press, Cambridge, 2004).

^[5] J. A. Smolin and D. P. DiVincenzo, Five two-bit quantum gates are sufficient to implement the quantum fredkin gate, Phys. Rev. A 53, 2855 (1996).

^[6] L. M. K. Vandersypen, M. Steffen, G. Breyta, C. S. Yannoni, M. H. Sherwood, and I. L. Chuang, Experimental realization of shor's quantum factoring algorithm using nuclear magnetic

- resonance, Nature (London) 414, 883 (2001).
- [7] E. Martín-López, A. Laing, T. Lawson, R. Alvarez, X.-Q. Zhou, and J. L. O'Brien, Experimental realization of shor's quantum factoring algorithm using qubit recycling, Nat. Photonics 6, 773 (2012).
- [8] B. P. Lanyon, T. J. Weinhold, N. K. Langford, M. Barbieri, D. F. V. James, A. Gilchrist, and A. G. White, Experimental Demonstration of a Compiled Version of Shor's Algorithm with Quantum Entanglement, Phys. Rev. Lett. 99, 250505 (2007).
- [9] H. Buhrman, R. Cleve, J. Watrous, and R. de Wolf, Quantum Fingerprinting, Phys. Rev. Lett. 87, 167902 (2001).
- [10] R. T. Horn, S. A. Babichev, K.-P. Marzlin, A. I. Lvovsky, and B. C. Sanders, Single-Qubit Optical Quantum Fingerprinting, Phys. Rev. Lett. 95, 150502 (2005).
- [11] I. L. Chuang and Y. Yamamoto, Quantum bit regeneration, Phys. Rev. Lett. 76, 4281 (1996).
- [12] A. Barenco, A. Berthiaume, D. Deutsch, A. Ekert, R. Jozsa, and C. Macchiavello, Stabilization of Quantum Computations by Symmetrization, SIAM J. Comp. 26, 1541 (1997).
- [13] A. K. Ekert, C. M. Alves, D. K. L. Oi, M. Horodecki, P. Horodecki, and L. C. Kwek, Direct Estimations of Linear and Nonlinear Functionals of a Quantum State, Phys. Rev. Lett. 88, 217901 (2002).
- [14] J. Fiurášek, M. Dušek, and R. Filip, Universal Measurement Apparatus Controlled by Quantum Software, Phys. Rev. Lett. 89, 190401 (2002).
- [15] R. B. Patel, J. Ho, F. Ferreyrol, T. C. Ralph, and G. J. Pryde, A quantum Fredkin gate, Sci. Adv. 2 (2016).
- [16] Y. Li, L. Wan, H. Zhang, H. Zhu, Y. Shi, L. K. Chin, X. Zhou, L. C. Kwek, and A. Q. Liu, Quantum fredkin and toffoli gates on a versatile programmable silicon photonic chip, NPJ Quantum Inf. 8 (2022).
- [17] M. Gong, S. Wang, C. Zha, M.-C. Chen, H.-L. Huang, Y. Wu, Q. Zhu, Y. Zhao, S. Li, S. Guo, H. Qian, Y. Ye, F. Chen, C. Ying, J. Yu, D. Fan, D. Wu, H. Su, H. Deng, H. Rong, K. Zhang, S. Cao, J. Lin, Y. Xu, L. Sun, C. Guo, N. Li, F. Liang, V. M. Bastidas, K. Nemoto, W. J. Munro, Y.-H. Huo, C.-Y. Lu, C.-Z. Peng, X. Zhu, and J.-W. Pan, Quantum walks on a programmable two-dimensional 62-qubit superconducting processor, Science 372, 948 (2021).
- [18] J. Carolan, C. Harrold, C. Sparrow, E. Martín-López, N. J. Russell, J. W. Silverstone, P. J. Shadbolt, N. Matsuda, M. Oguma, M. Itoh, G. D. Marshall, M. G. Thompson, J. C. F. Matthews, T. Hashimoto, J. L. O'Brien, and A. Laing, Universal linear optics, Science 349, 711 (2015).
- [19] S. Ebadi, T. T. Wang, H. Levine, A. Keesling, G. Semeghini, A. Omran, D. Bluvstein, R. Samajdar, H. Pichler, W. W. Ho, S. Choi, S. Sachdev, M. Greiner, V. Vuletić, and M. D. Lukin, Quantum phases of matter on a 256-atom programmable quantum simulator, Nature (London) 595, 227 (2021).
- [20] A. Reiserer and G. Rempe, Cavity-based quantum networks with single atoms and optical photons, Rev. Mod. Phys. 87, 1379 (2015).
- [21] T. Pellizzari, S. A. Gardiner, J. I. Cirac, and P. Zoller, Decoherence, Continuous Observation, and Quantum Computing: A Cavity QED Model, Phys. Rev. Lett. 75, 3788 (1995).
- [22] J. I. Cirac, P. Zoller, H. J. Kimble, and H. Mabuchi, Quantum State Transfer and Entanglement Distribution among Distant Nodes in a Quantum Network, Phys. Rev. Lett. 78, 3221 (1997).
- [23] L.-M. Duan and H. J. Kimble, Scalable Photonic Quantum Computation through Cavity-Assisted Interactions, Phys. Rev. Lett. 92, 127902 (2004).
- [24] H. J. Kimble, The quantum internet, Nature (London) 453, 1023 (2008).

- [25] C. Monroe, Quantum information processing with atoms and photons, Nature (London) 416, 9 (2002).
- [26] S. Ritter, C. Nölleke, C. Hahn, A. Reiserer, A. Neuzner, M. Uphoff, M. Mücke, E. Figueroa, J. Bochmann, and G. Rempe, An elementary quantum network of single atoms in optical cavities, Nature (London) 484, 195 (2012).
- [27] M. Brekenfeld, D. Niemietz, J. D. Christesen, and G. Rempe, A quantum network node with crossed optical fibre cavities, Nat. Phys. 16, 647 (2020).
- [28] V. Scarani, H. Bechmann-Pasquinucci, N. J. Cerf, M. Dušek, N. Lütkenhaus, and M. Peev, The security of practical quantum key distribution, Rev. Mod. Phys. 81, 1301 (2009).
- [29] S. Langenfeld, P. Thomas, O. Morin, and G. Rempe, Quantum Repeater Node Demonstrating Unconditionally Secure Key Distribution, Phys. Rev. Lett. 126, 230506 (2021).
- [30] K. S. Choi, H. Deng, J. Laurat, and H. J. Kimble, Mapping photonic entanglement into and out of a quantum memory, Nature (London) 453, 67 (2008).
- [31] S. Langenfeld, O. Morin, M. Körber, and G. Rempe, A network-ready random-access qubits memory, NPJ Quantum Inf. 6, 10.1038/s41534-020-00316-8 (2020).
- [32] S. Langenfeld, S. Welte, L. Hartung, S. Daiss, P. Thomas, O. Morin, E. Distante, and G. Rempe, Quantum teleportation between remote qubit memories with only a single photon as a resource, Phys. Rev. Lett. 126, 130502 (2021).
- [33] D. Tiarks, S. Baur, K. Schneider, S. Dürr, and G. Rempe, Single-Photon Transistor Using a Förster Resonance, Phys. Rev. Lett. 113, 053602 (2014).
- [34] Q. A. Turchette, C. J. Hood, W. Lange, H. Mabuchi, and H. J. Kimble, Measurement of Conditional Phase Shifts for Quantum Logic, Phys. Rev. Lett. 75, 4710 (1995).
- [35] L.-M. Duan, B. Wang, and H. J. Kimble, Robust quantum gates on neutral atoms with cavity-assisted photon scattering, Phys. Rev. A 72, 032333 (2005).
- [36] Y. L. Zhou and C. Z. Li, Robust quantum gates via a photon triggering electromagnetically induced transparency, Phys. Rev. A 84, 044304 (2011).
- [37] H. S. Borges and C. J. Villas-Bôas, Quantum phase gate based on electromagnetically induced transparency in optical cavities, Phys. Rev. A 94, 052337 (2016).
- [38] H. S. Borges, D. Z. Rossatto, F. S. Luiz, and C. J. Villas-Boas, Heralded entangling quantum gate via cavity-assisted photon scattering, Phys. Rev. A 97, 013828 (2018).
- [39] B. Hacker, S. Welte, G. Rempe, and S. Ritter, A photon-photon quantum gate based on a single atom in an optical resonator, Nature (London) 536, 193 (2016).
- [40] S. Daiss, S. Langenfeld, S. Welte, E. Distante, P. Thomas, L. Hartung, O. Morin, and G. Rempe, A quantum-logic gate between distant quantum-network modules, Science 371, 614 (2021).
- [41] T. Stolz, H. Hegels, M. Winter, B. Röhr, Y.-F. Hsiao, L. Husel, G. Rempe, and S. Dürr, Quantum-Logic Gate between Two Optical Photons with an Average Efficiency above 40%, Phys. Rev. X 12, 021035 (2022).
- [42] S. H. Autler and C. H. Townes, Stark Effect in Rapidly Varying Fields, Phys. Rev. 100, 703 (1955).
- [43] M. Fleischhauer, A. Imamoglu, and J. P. Marangos, Electromagnetically induced transparency: Optics in coherent media, Rev. Mod. Phys. 77, 633 (2005).
- [44] P. M. Alsing, D. A. Cardimona, and H. J. Carmichael, Suppression of fluorescence in a lossless cavity, Phys. Rev. A 45, 1793 (1992).
- [45] P. Rice and R. Brecha, Cavity induced transparency, Opt. Commun. 126, 230 (1996).

- [46] C. Gardiner and P. Zoller, Quantum Noise: A Handbook of Markovian and Non-Markovian Quantum Stochastic Methods with Applications to Quantum Optics (Springer-Verlag, Berlin, 2010).
- [47] R. Loudon, *The Quantum Theory of Light* (Oxford University Press, Oxford, 2000).
- [48] D. Walls and G. Milburn, *Quantum Optics* (Springer Berlin Heidelberg, 2008).
- [49] H. Primakoff and T. Holstein, Many-Body Interactions in Atomic and Nuclear Systems, Phys. Rev. 55, 1218 (1939).
- [50] See Supplemental Material at [URL will be inserted by publisher] for details.
- [51] R. Bonifacio and G. Preparata, Coherent Spontaneous Emission, Phys. Rev. A 2, 336 (1970).
- [52] J. Dilley, P. Nisbet-Jones, B. W. Shore, and A. Kuhn, Single-photon absorption in coupled atom-cavity systems, Phys. Rev. A 85, 023834 (2012).

- [53] B. Q. Baragiola, R. L. Cook, A. M. Brańczyk, and J. Combes, N-photon wave packets interacting with an arbitrary quantum system, Phys. Rev. A **86**, 013811 (2012).
- [54] Here, we assume that τ_p is sufficiently long to ensure that the pulse spectral spread (τ_p^{-1}) fits within the linewidth of the cavity (2κ) , i.e., the entire input pulse enters and exits the cavity, resulting in an output pulse that maintains the shape of the input pulse. [38].
- [55] S. M. Barnett, J. Jeffers, A. Gatti, and R. Loudon, Quantum optics of lossy beam splitters, Phys. Rev. A 57, 2134 (1998).
- [56] M. Delanty, S. Rebic, and J. Twamley, Superradiance of harmonic oscillators (2011), arXiv:1107.5080.
- [57] C. E. Máximo, P. P. de Souza, C. Ianzano, G. Rempe, R. Bachelard, and C. J. Villas-Boas, Bright and Dark States of Light: The Quantum Origin of Classical Interference (2021), arXiv:2112.05512.
- [58] A. Blais, A. L. Grimsmo, S. M. Girvin, and A. Wallraff, Circuit quantum electrodynamics, Rev. Mod. Phys. 93, 025005 (2021).

Supplemental Material for Universal Quantum Computation Using Atoms in Cross-Cavity Systems

Luiz Otavio Ribeiro Solak, Daniel Zini Rossatto, and Celso Jorge Villas-Boas I

¹Departamento de Física, Universidade Federal de São Carlos, 13565-905 São Carlos, São Paulo, Brazil

²Universidade Estadual Paulista (Unesp), Instituto de Ciências e Engenharia, Campus de Itapeva, 18409-010 Itapeva, São Paulo, Brazil

I. HEISENBERG-LANGEVIN EQUATIONS WITH HOLSTEIN-PRIMAKOFF APPROXIMATION: ANALYTICAL METHOD

Consider crossed optical cavities coupled to a Λ -type three-level atom (two metastable ground states, $|g_1\rangle$ and $|g_2\rangle$, and an excited one $|e\rangle$). Each cavity is single sided with their semitransparent mirrors coupled to a continuum of free-space modes (bosonic reservoir). Moreover, each atomic transition, $|g_1\rangle \leftrightarrow |e\rangle$ and $|g_2\rangle \leftrightarrow |e\rangle$, interacts with its respective reservoir. This setup can be described, in an interaction picture rotating at the cavity frequency (ω_c), and under the *white-noise limit*, by the Hamiltonian ($\hbar = 1$) [1]

$$H = \int_{-\infty}^{\infty} d\omega \omega A_{\omega}^{\dagger} A_{\omega} + \int_{-\infty}^{\infty} d\omega \omega B_{\omega}^{\dagger} B_{\omega} + \int_{-\infty}^{\infty} d\omega \omega C_{\omega}^{\dagger} C_{\omega} + \int_{-\infty}^{\infty} d\omega \omega D_{\omega}^{\dagger} D_{\omega}$$

$$+ \frac{i}{\sqrt{2\pi}} \int_{-\infty}^{\infty} d\omega \left[\sqrt{2\kappa_{a}} (a^{\dagger} A_{\omega} - a A_{\omega}^{\dagger}) \right] + \frac{i}{\sqrt{2\pi}} \int_{-\infty}^{\infty} d\omega \left[\sqrt{2\kappa_{b}} (b^{\dagger} B_{\omega} - b B_{\omega}^{\dagger}) \right]$$

$$+ \frac{i}{\sqrt{2\pi}} \int_{-\infty}^{\infty} d\omega \left[\sqrt{2\Gamma_{1}} (C_{\omega} \sigma_{+}^{1} - C_{\omega}^{\dagger} \sigma_{-}^{1}) \right] + \frac{i}{\sqrt{2\pi}} \int_{-\infty}^{\infty} d\omega \left[\sqrt{2\Gamma_{2}} (D_{\omega} \sigma_{+}^{2} - D_{\omega}^{\dagger} \sigma_{-}^{2}) \right]$$

$$+ \underbrace{(g_{a} a + g_{b} b) \sigma_{+}^{1} + (g_{a}^{*} a^{\dagger} + g_{b} b^{*\dagger}) \sigma_{-}^{1}}_{H_{sys}}, \tag{1}$$

where $\sigma_+^j = |e\rangle\langle g_j|$ and $\sigma_-^j = |g_j\rangle\langle e|$ are atomic ladder operators, a and b (a^\dagger and b^\dagger) are the annihilation (creation) operators of the intracavity modes, while A_ω and B_ω (A_ω^\dagger and B_ω^\dagger) are the frequency-dependent annihilation (creation) operators [2] of the bosonic reservoirs of cavities a and b, respectively. The decay rates of the field amplitudes of cavities a and b are represented by κ_a and κ_b , respectively. Similarly, the atomic reservoirs are determined by the frequency-dependent bosonic operators C_ω and D_ω , which are responsible for the atomic decay from $|e\rangle$ to $|g_1\rangle$ and $|g_2\rangle$ with rates Γ_1 and Γ_2 , respectively. Finally, g_a and g_b stand for the coupling strength between the atomic transition $|g_1\rangle \leftrightarrow |e\rangle$ and the intracavity modes, while the atomic ground state $|g_2\rangle$ remains uncoupled. Consequently, the atom remains unchanged when initially in the state $|g_2\rangle$. Thus, the atom becomes transparent to the cavities, resulting in an empty-cavity scenario. In this case, the dynamics can be obtained from H by setting $g_a = g_b = 0$.

The Heisenberg-Langevin equation for an arbitrary system operator $\mathcal{O}(t)$ is written as [1]

$$\dot{\mathcal{O}} = -i[\mathcal{O}, H_{\text{sys}}] - \sum_{l=1}^{2} \Gamma_{l}([\mathcal{O}, \sigma_{+}^{l}] \sigma_{-}^{l} - \sigma_{+}^{l}[\mathcal{O}, \sigma_{-}^{l}])
- \sum_{z=a}^{b} [\mathcal{O}, z^{\dagger}] (\kappa_{z} z - \sqrt{2\kappa_{z}} z_{\text{in}})
+ \sum_{z=a}^{b} (\kappa_{z} z^{\dagger} - \sqrt{2\kappa_{z}} z_{\text{in}}^{\dagger}) [\mathcal{O}, z],$$
(2)

in which we have the input and output operators [3]

$$z_{\text{out}}(t) = +\frac{1}{\sqrt{2\pi}} \int_{-\infty}^{\infty} d\omega e^{-i\omega(t - t_{\text{out}})} \underbrace{Z_{\omega}(t_{\text{out}})}_{z_{\text{out}}(\omega)}, \tag{3}$$

$$z_{\rm in}(t) = -\frac{1}{\sqrt{2\pi}} \int_{-\infty}^{\infty} d\omega e^{-i\omega(t - t_{\rm in})} \underbrace{Z_{\omega}(t_{\rm in})}_{z_{\rm in}(\omega)},\tag{4}$$

which are related to each other through the input-output relation

$$z_{\text{out}}(t) = \sqrt{2\kappa_z} z(t) - z_{\text{in}}(t), \tag{5}$$

for $\{z=a,Z=A\}$ and $\{z=b,Z=B\}$. It is important stressing that, without loss of generality, we suppress in Eq (2) the input operators for the atomic reservoirs as they are assumed to be initially in the vacuum state.

From Eq. (2), the resulting dynamical equations for the system operators are

$$\dot{a}(t) = -ig_a^* \sigma_-^1(t) - \kappa_a a(t) + \sqrt{2\kappa_a} a_{\rm in}(t), \tag{6}$$

$$\dot{b}(t) = -ig_b^* \sigma_-^1(t) - \kappa_b b(t) + \sqrt{2\kappa_b} b_{\rm in}(t), \tag{7}$$

$$\dot{\sigma}_{-}^{1}(t) = i[g_{a}a(t) + g_{b}b(t)]\sigma_{z}(t) - \Gamma\sigma_{-}^{1}(t), \tag{8}$$

with $\Gamma = \Gamma_1 + \Gamma_2$. This set of coupled differential equations can be linearized by applying the Holstein-Primakoff approximation $\sigma_z = \sigma_+^1 \sigma_-^1 - \sigma_-^1 \sigma_+^1 \approx -1$ [4], which holds as long as the atom is rarely excited. On the other hand, this approximation is indeed exact when the atom exclusively populates $|g_2\rangle$ or when $g_a = g_b = 0$ (both cases are equivalent). Thus,

$$\dot{a}(t) = -ig_a^* \sigma_-^1(t) - \kappa_a a(t) + \sqrt{2\kappa_a} a_{\rm in}(t), \tag{9}$$

$$\dot{b}(t) = -ig_b^* \sigma_-^1(t) - \kappa_b b(t) + \sqrt{2\kappa_b} b_{\rm in}(t), \tag{10}$$

$$\dot{\sigma}_{-}^{1}(t) = -i[g_{a}a(t) + g_{b}b(t)] - \Gamma\sigma_{-}^{1}(t). \tag{11}$$

The Fourier transform of Eqs. (9)–(11) yields

$$-i\omega a(\omega) = -ig_a^* \sigma_-^1(\omega) - \kappa_a a(\omega) + \sqrt{2\kappa_a} a_{\rm in}(\omega); \tag{12}$$

$$-i\omega b(\omega) = -ig_b^* \sigma_-^1(\omega) - \kappa_b b(\omega) + \sqrt{2\kappa_b} b_{\rm in}(\omega);$$
(13)

$$-i\omega\sigma_{-}^{1}(\omega) = -i[g_{a}a(\omega) + g_{b}b(\omega)] - \Gamma\sigma_{-}^{1}(t).$$
(14)

Considering just for convenience $g_a = -g_b \equiv g \in \mathbb{R}$ and $\kappa_a = \kappa_b \equiv \kappa$, we have from Eq. (14) that

$$\sigma_{-}^{1}(\omega) = -\frac{ig}{\Gamma - i\omega}(a(\omega) - b(\omega)) = -\frac{ig\sqrt{2}}{(\Gamma - i\omega)}X^{-}(\omega), \tag{15}$$

where the collective-mode operators are defined as

$$X^{\pm}(\omega) = \frac{1}{\sqrt{2}}[a(\omega) \pm b(\omega)]. \tag{16}$$

We must be cautious when expressing the atomic operator in terms of the collective-mode operator [Eq. (15)] to be inserted into Eqs. (12) and (13), since there is a risk of overlooking a proper description of the information regarding the atom. Specifically, by performing this substitution, we disregard the fact that $\sigma_{-}^{1}(\omega) = 0$ in Eq. (15) when the atom is initially in $|g_2\rangle$ (which

is equivalent to g=0). For our purpose, this mistake can be avoided by considering in an ad hoc manner the substitution $g \to \tilde{g} = g|g_1\rangle\langle g_1|$ in the right side of Eq. (15).

Inserting Eq. (15) into Eqs. (12) and (13),

$$X^{-}(\omega) = \frac{\sqrt{2\kappa}(\Gamma - i\omega)}{(\kappa - i\omega)(\Gamma - i\omega) + (\tilde{g}\sqrt{2})^{2}} X_{\rm in}^{-}(\omega), \tag{17}$$

$$X^{+}(\omega) = \frac{\sqrt{2\kappa}}{\kappa - i\omega} X_{+}^{\text{in}}(\omega), \tag{18}$$

where we can observe that the symmetric collective-mode operator are decoupled from the atom regardless its state, since it does not depend on g. From the input-output relation written in terms of the collective-mode operators, $X_{\text{out}}^{\pm}(\omega) = \sqrt{2\kappa}X^{\pm}(\omega) - X_{\text{in}}^{\pm}(\omega)$, we obtain

$$X_{\text{out}}^{-}(\omega) = x_{-}^{*}X_{\text{in}}^{-}(\omega),\tag{19}$$

$$X_{\text{out}}^{+}(\omega) = x_{+}^{*} X_{\text{in}}^{+}(\omega),$$
 (20)

with

$$x_{-}^{*} \equiv \frac{(\kappa + i\omega)(\Gamma - i\omega) - (\tilde{g}\sqrt{2})^{2}}{(\kappa - i\omega)(\Gamma - i\omega) + (\tilde{g}\sqrt{2})^{2}},\tag{21}$$

$$x_{+}^{*} \equiv \left(\frac{\kappa + i\omega}{\kappa - i\omega}\right),\tag{22}$$

directly implying in

$$a_{\text{out}}^{\dagger}(\omega) = \underbrace{\frac{(x_{+} + x_{-})}{2}}_{r_{\omega}} a_{\text{in}}^{\dagger}(\omega) + \underbrace{\frac{(x_{+} - x_{-})}{2}}_{t_{\omega}} b_{\text{in}}^{\dagger}(\omega), \tag{23}$$

$$b_{\text{out}}^{\dagger}(\omega) = \underbrace{\frac{(x_{+} - x_{-})}{2}}_{t_{\text{tot}}} a_{\text{in}}^{\dagger}(\omega) + \underbrace{\frac{(x_{+} + x_{-})}{2}}_{T_{\text{tot}}} b_{\text{in}}^{\dagger}(\omega), \tag{24}$$

with r_{ω} and t_{ω} being the (frequency- and atomic-state-dependent) complex reflection and transmission coefficients.

At this point it is important remarking that the Hamiltonian in Eq. (1) was written in an interaction picture rotating at the cavities frequency. The results for the Heisenberg picture are obtained by making $\omega \to \omega - \omega_c$ in Eqs. (19) and (20). Therefore, the system response for resonant incoming fields ($\omega = \omega_c$) can be explicitly written as

$$r_{\omega=\omega_c} = \frac{1}{1+4C} |g_1\rangle\langle g_1| + |g_2\rangle\langle g_2|, \tag{25}$$

$$t_{\omega=\omega_c} = \frac{4C}{1+4C} |g_1\rangle\langle g_1|,\tag{26}$$

in which $C = g^2/2\kappa\Gamma$ is the cooperativity parameter.

II. MEAN-FIELD APPROXIMATION: SEMICLASSICAL METHOD

When the atom can be significantly excited, in a parameter regime beyond the validity of the Holstein-Primakoff approximation, it is convenient to work with the dynamical equations for the expectation values of the operators in Eqs. (6)–(8)

$$\langle \dot{a} \rangle = -ig_a^* \langle \sigma_-^1 \rangle - \kappa_a \langle a \rangle + \sqrt{2\kappa_a} \langle a_{\rm in} \rangle, \tag{27}$$

$$\langle \dot{b} \rangle = -ig_b^* \langle \sigma_-^1 \rangle - \kappa_b \langle b \rangle + \sqrt{2\kappa_b} \langle b_{\rm in} \rangle, \tag{28}$$

$$\langle \dot{\sigma}_{-}^{1} \rangle = i(g_a \langle a\sigma_z \rangle + g_b \langle b\sigma_z \rangle) - \Gamma \langle \sigma_{-}^{1} \rangle. \tag{29}$$

This set of differential equations is not closed. Specifically, the equation of motion for $\langle \sigma_-^1 \rangle$ depends on the expectation values $\langle a\sigma_z \rangle$ and $\langle b\sigma_z \rangle$, which involve two operators. Similarly, the equations of motion for expectation values involving two operators rely on expectation values with three operators, and so forth (known as Bogoliubov-Born-Green-Kirkwood-Yvon (BBGKY) hierarchy [5]). An approach to truncate this set of equations, beyond the Holstein-Primakoff approximation, is through the semiclassical mean-field approximation [6], which relies on the factorization of expectation values that involve two operators, e.g., $\langle \sigma a \rangle \approx \langle \sigma \rangle \langle a \rangle$. The resulting set of dynamical equations becomes finite but nonlinear

$$\langle \dot{a} \rangle = -ig_a^* \langle \sigma_-^1 \rangle - \kappa_a \langle a \rangle + \sqrt{2\kappa_a} \langle a_{\rm in} \rangle, \tag{30}$$

$$\langle \dot{b} \rangle = -ig_b^* \langle \sigma_-^1 \rangle - \kappa_b \langle b \rangle + \sqrt{2\kappa_b} \langle b_{\rm in} \rangle, \tag{31}$$

$$\langle \dot{\sigma_{-}}^{1} \rangle = i(g_a \langle a \rangle + g_b \langle b \rangle) \langle \sigma_z \rangle - \Gamma \langle \sigma_{-}^{1} \rangle, \tag{32}$$

$$\langle \dot{\sigma}_z \rangle = -2i(g_a \langle a \rangle + g_b \langle b \rangle) \langle \sigma_-^1 \rangle^* + 2i(g_a^* \langle a \rangle^* + g_b^* \langle b \rangle^*) \langle \sigma_-^1 \rangle - 2(\Gamma_1 + \Gamma) \langle \sigma_{ee} \rangle, \tag{33}$$

$$\langle \dot{\sigma_{ee}} \rangle = -i(g_a \langle a \rangle + g_b \langle b \rangle) \langle \sigma_-^1 \rangle^* + i(g_a^* \langle a \rangle^* + g_b^* \langle b \rangle^*) \langle \sigma_-^1 \rangle - 2\Gamma \langle \sigma_{ee} \rangle, \tag{34}$$

with $\sigma_{ee} = |e\rangle\langle e|$. The solution to the semiclassical dynamical equations can be obtained numerically without difficulty, even if there are many atoms inside the cross-cavity setup. Nonetheless, this solution neglects the correlation between the atom and the intracavity fields, and assumes the external fields as classical ones (coherent pulses), such that $\langle a_{\rm in} \rangle = \alpha_{\rm in}(t)$ and $\langle b_{\rm in} \rangle = \beta_{\rm in}(t)$, where $\alpha_{\rm in}(t)$ are the square-normalized temporal shapes of the incoming pulses impinging upon the cavities a and b, respectively.

III. SCHRÖDINGER EQUATION FOR SINGLE-EXCITATION INITIAL STATE: EXACT METHOD

When the initial state of the setup contains a single excitation

$$|\Psi(t_0)\rangle = (\lambda_1|g_1\rangle + \lambda_2|g_2\rangle) \otimes (|0\rangle_a \otimes |0\rangle_b) \otimes (\mu_a|1\rangle_\alpha \otimes |0\rangle_\beta + \mu_b|0\rangle_\alpha \otimes |1\rangle_\beta), \tag{35}$$

an exact solution can be obtained by numerically solving the Schrödinger equation $i\partial_t |\Psi(t)\rangle = H_{\rm eff} |\Psi(t)\rangle$, with $H_{\rm eff} = H - i\Gamma\sigma_{ee}$ [7]. Here $|1\rangle_{\alpha} = \int_{-\infty}^{\infty} d\omega \xi_{\rm in}(\omega) A_{\omega}^{\dagger} |0\rangle_{\alpha}$ describes the input field in a continuous-mode single-photon state [2] impinging upon the cavity a, and $|1\rangle_{\beta} = \int_{-\infty}^{\infty} d\omega \zeta_{\rm in}(\omega) B_{\omega}^{\dagger} |0\rangle_{\beta}$ the analog for cavity b. The Fourier transform of the spectral density function of the pulses, $\xi_{\rm in}(\omega)$ and $\zeta_{\rm in}(\omega)$, gives the square-normalized temporal shape of the incoming pulses, $\alpha_{\rm in}(t)$ and $\beta_{\rm in}(t)$, respectively. Finally λ_k , k=1, 2 and μ_p , for p=a, b, will determine the initial occupation of the system states.

The non-Hermitian damping term, $-i\Gamma\sigma_{ee}$, excludes the occurrences of photon loss due to spontaneous atomic emission, replacing the reservoirs previously considered, such that

$$H_{\text{eff}} = \int_{-\infty}^{\infty} d\omega \omega A_{\omega}^{\dagger} A_{\omega} + \int_{-\infty}^{\infty} d\omega \omega B_{\omega}^{\dagger} B_{\omega}$$

$$+ \frac{i}{\sqrt{2\pi}} \int_{-\infty}^{\infty} d\omega \left[\sqrt{2\kappa_{a}} (a^{\dagger} A_{\omega} - a A_{\omega}^{\dagger}) \right] + \frac{i}{\sqrt{2\pi}} \int_{-\infty}^{\infty} d\omega \left[\sqrt{2\kappa_{b}} (b^{\dagger} B_{\omega} - b B_{\omega}^{\dagger}) \right]$$

$$+ (g_{a} a + g_{b} b) \sigma_{+} + (g_{a}^{*} a^{\dagger} + g_{b}^{*} b^{\dagger}) \sigma_{-} - i \Gamma \sigma_{ee}.$$
(36)

This non-Hermitian nature of $H_{\rm eff}$ results in an unnormalized state $|\Psi(t)\rangle$, such that $\int_{-\infty}^{\infty} |\langle \Psi(t)|\Psi(t)\rangle|^2 dt$ quantifies the probability of not losing the input single photon due to atomic spontaneous emission.

The single excitation condition allows one to consider the following general evolved state

$$|\Psi(t)\rangle = c_{e}(t)|e\rangle|0\rangle_{a}|0\rangle_{b}|0\rangle_{\alpha}|0\rangle_{\beta}$$

$$+ \sum_{l=1}^{2} c_{a}^{l}(t)|g_{l}\rangle|1\rangle_{a}|0\rangle_{b}|0\rangle_{\alpha}|0\rangle_{\beta}$$

$$+ \sum_{l=1}^{2} c_{b}^{l}(t)|g_{l}\rangle|0\rangle_{a}|1\rangle_{b}|0\rangle_{\alpha}|0\rangle_{\beta}$$

$$+ \sum_{l=1}^{2} \int_{-\infty}^{\infty} d\omega \xi_{l}(\omega, t)|g_{l}\rangle|0\rangle_{a}|0\rangle_{b}A^{\dagger}(\omega)|0\rangle_{\alpha}|0\rangle_{\beta}$$

$$+ \sum_{l=1}^{2} \int_{-\infty}^{\infty} d\omega \zeta_{l}(\omega, t)|g_{l}\rangle|0\rangle_{a}|0\rangle_{b}|0\rangle_{\alpha}B^{\dagger}(\omega)|0\rangle_{\beta},$$
(37)

Inserting the evolved state $(|\Psi(t)\rangle)$ into the Schrödinger equation $i\partial_t |\Psi(t)\rangle = H_{\rm eff} |\Psi(t)\rangle$ yields the following sets of coupled integro-differential equations for the amplitudes

$$\begin{bmatrix} \dot{c}_e \\ \dot{c}_a^1 \\ \dot{c}_b^1 \\ \dot{\xi}_1 \\ \dot{\zeta}_1 \end{bmatrix} = \begin{bmatrix} -\Gamma & -ig_a & -ig_b & 0 & 0 \\ -ig_a^* & 0 & 0 & \sqrt{\kappa_a/\pi} \int d\omega & 0 \\ 0 & -ig_b^* & 0 & 0 & \sqrt{\kappa_b/\pi} \int d\omega \\ 0 & -\sqrt{\kappa_a/\pi} & 0 & -i\omega & 0 \\ 0 & 0 & -\sqrt{\kappa_b/\pi} & 0 & -i\omega \end{bmatrix} \begin{bmatrix} c_e \\ c_a^1 \\ c_b^1 \\ \xi_1 \\ \zeta_1 \end{bmatrix},$$
(38)

$$\begin{bmatrix} \dot{c}_a^2 \\ \dot{\xi}_2 \end{bmatrix} = \begin{bmatrix} 0 & \sqrt{\kappa_a/\pi} \int d\omega \\ \sqrt{\kappa_a/\pi} & -i\omega \end{bmatrix} \begin{bmatrix} c_a^2 \\ \xi_2 \end{bmatrix}, \tag{39}$$

$$\begin{bmatrix} \dot{c}_b^2 \\ \dot{\zeta}_2 \end{bmatrix} = \begin{bmatrix} 0 & \sqrt{\kappa_b/\pi} \int d\omega \\ \sqrt{\kappa_b/\pi} & -i\omega \end{bmatrix} \begin{bmatrix} c_b^2 \\ \zeta_2 \end{bmatrix}. \tag{40}$$

By integrating the equations for $\dot{\xi}_l$ and $\dot{\zeta}_l$ from an initial time t_0 to $t > t_0$, we obtain

$$\xi_l(\omega, t) = \xi_l(\omega, t_0) e^{-i\omega(t - t_0)} - \sqrt{\frac{\kappa_a}{\pi}} \int_{t_0}^t d\tau c_a^l(\tau) e^{-i\omega(t - \tau)}, \tag{41}$$

$$\zeta_l(\omega, t) = \zeta_l(\omega, t_0) e^{-i\omega(t - t_0)} - \sqrt{\frac{\kappa_b}{\pi}} \int_{t_0}^t d\tau c_b^l(\tau) e^{-i\omega(t - \tau)}, \tag{42}$$

for l=1,2. Now we apply the time limit for these solutions, for a past time $t_0 \longrightarrow -\infty$ we obtain $\xi_l(\omega,t_0) \equiv \xi_{\rm in}^l(\omega)$ and $\zeta_l(\omega,t_0) \equiv \zeta_{\rm in}^l(\omega)$ where the incoming pulse is still at sufficiently large distance from the cavity. Also, we integrate for t to a future time $t_1 > t$, such that

$$\xi_l(\omega, t) = \xi_l(\omega, t_1) e^{-i\omega(t - t_1)} - \sqrt{\frac{\kappa_a}{\pi}} \int_t^{t_1} d\tau c_a^l(\tau) e^{-i\omega(t - \tau)}, \tag{43}$$

$$\zeta_l(\omega, t) = \zeta_l(\omega, t_1) e^{-i\omega(t - t_1)} - \sqrt{\frac{\kappa_b}{\pi}} \int_t^{t_1} d\tau c_b^l(\tau) e^{-i\omega(t - \tau)}. \tag{44}$$

Similarly for a future time $t_1 \to +\infty$, we obtain $\xi_l(\omega, t_1) \equiv -\xi_{\text{out}}^l$ and $\zeta_l(\omega_1, t_1) \equiv -\zeta_{\text{out}}^l$, where the minus sign comes from the convention that takes into account the propagation direction of the fields in their amplitudes.

The square-normalized temporal shapes of the incoming and outgoing pulses related to cavity a are

$$\alpha_{\rm in}^l(t) = \frac{1}{\sqrt{2\pi}} \int_{-\infty}^{+\infty} \xi_{\rm in}(\omega) e^{-i\omega(t-t_0)},\tag{45}$$

$$\alpha_{\text{out}}^{l}(t) = \frac{1}{\sqrt{2\pi}} \int_{-\infty}^{+\infty} \xi_{\text{out}}(\omega) e^{-i\omega(t-t_1)},\tag{46}$$

and similar for $\beta_{\rm in,out}^l(t)$ with $\zeta_{\rm in,out}^l$. As a result, combining the Eqs. (45) and (46) with the relations obtained for $\xi_l(\omega,t)$ and $\zeta_l(\omega,t)$, we obtain

$$\alpha_{\text{out}}^l(t) = \sqrt{2\kappa_a} c_a^l(t) - \alpha_{\text{in}}^l(t), \tag{47}$$

$$\beta_{\text{out}}^l(t) = \sqrt{2\kappa_b} c_b^l(t) - \beta_{\text{in}}^l(t). \tag{48}$$

which are the boundary conditions relating the field amplitudes outside the cavities to the intracavity fields.

The last step to build a solvable set of equations is to eliminate the integral terms in $\dot{c}_a^l(t)$ and $\dot{c}_b^l(t)$. Let us take as an example the equation for $\dot{c}_a^l(t)$,

$$\dot{c}_{a}^{l}(t) = -ig_{a}^{*}\delta_{l,1}c_{e} + \sqrt{\frac{\kappa_{a}}{\pi}} \int_{-\infty}^{+\infty} d\omega \xi_{l}(\omega, t)$$

$$= -ig_{a}^{*}\delta_{l,1}c_{e} + \sqrt{\frac{\kappa_{a}}{\pi}} \int_{-\infty}^{+\infty} d\omega \left[\xi_{\text{in}}^{l}(\omega)e^{-i\omega(t-t_{0})} - \sqrt{\frac{\kappa_{a}}{\pi}} \int_{t_{0}}^{t} d\tau c_{a}^{l}(\tau)e^{-i\omega(t-\tau)} \right]$$

$$= -ig_{a}^{*}\delta_{l,1}c_{e} + \sqrt{\frac{\kappa_{a}}{\pi}} \underbrace{\int_{-\infty}^{+\infty} d\omega \xi_{\text{in}}^{l}(\omega)e^{-i\omega(t-t_{0})}}_{\sqrt{2\pi}\alpha_{\text{in}}^{l}(t)} - \underbrace{\frac{\kappa_{a}}{\pi} \int_{t_{0}}^{t} d\tau c_{a}^{l}(\tau) \underbrace{\int_{-\infty}^{+\infty} d\omega e^{-\omega(t-\tau)}}_{2\pi\delta(t-\tau)}, \tag{49}$$

such that

$$\dot{c}_a^l(t) = -ig_a^* \delta_{l,1} c_e + \sqrt{2\kappa_a} \alpha_{\rm in}^l(t) - \kappa_a c_a^l(t). \tag{50}$$

The same procedure can be taken for $c_h^l(t)$, yielding the following set of coupled differential equations

$$\dot{c}_{a}^{1}(t) = -ig_{a}^{*}c_{e}(t) - \kappa_{a}c_{a}^{1}(t) + \sqrt{2\kappa_{a}}\alpha_{\text{in}}^{1}(t); \qquad \dot{c}_{a}^{2} = -\kappa_{a}c_{a}^{2}(t) + \sqrt{2\kappa_{a}}\alpha_{\text{in}}^{2}(t);
\dot{c}_{b}^{1}(t) = -ig_{b}^{*}c_{e}(t) - \kappa_{b}c_{b}^{1}(t) + \sqrt{2\kappa_{b}}\beta_{\text{in}}^{1}(t); \qquad \dot{c}_{b}^{2} = -\kappa_{b}c_{b}^{2}(t) + \sqrt{2\kappa_{b}}\beta_{\text{in}}^{2}(t);
\dot{c}_{e}(t) = -\Gamma c_{e}(t) - ig_{a}c_{a}^{1}(t) - ig_{b}c_{b}^{1}(t). \qquad (51)$$

Given a certain input pulse $[\alpha_{\rm in}(t)]$ and $\beta_{\rm in}(t)$ and consider the initial state of Eq. (35), we have that $\alpha_{\rm in}^l(t) = \lambda_l \mu_a \alpha_{\rm in}(t)$, $\beta_{\rm in}^l(t) = \lambda_l \mu_b \beta_{\rm in}(t)$ and $c_a^l(0) = c_b^l(0) = 0$. Then, it is straightforward to numerically solve the system dynamics and hence access the outgoing pulse dynamics through $\alpha_{\rm out}^l(t)$ and $\beta_{\rm out}^l(t)$ determined by Eqs. (47) and (48).

^[1] C. Gardiner and P. Zoller, Quantum Noise: A Handbook of Markovian and Non-Markovian Quantum Stochastic Methods with Applications to Quantum Optics (Springer-Verlag, Berlin, 2010).

^[2] R. Loudon, *The Quantum Theory of Light* (Oxford University Press, Oxford, 2000).

^[3] D. Walls and G. Milburn, Quantum Optics (Springer Berlin Heidelberg, 2008).

^[4] H. Primakoff and T. Holstein, Many-Body Interactions in Atomic and Nuclear Systems, Phys. Rev. 55, 1218 (1939).

- [5] M. Bonitz, Quantum kinetic theory, Vol. 412 (Springer, Heidelberg, 2016).
- [6] R. Bonifacio and G. Preparata, Coherent Spontaneous Emission, Phys. Rev. A 2, 336 (1970).
- [7] J. Dilley, P. Nisbet-Jones, B. W. Shore, and A. Kuhn, Single-photon absorption in coupled atom-cavity systems, Phys. Rev. A 85, 023834 (2012).